

1 **Potential function of *CbuSPL* and gene encoding its interacting protein during flowering in**

2 ***Catalpa bungei***

3 Zhi Wang<sup>1</sup>, Tianqing Zhu<sup>1</sup>, Erqin Fan<sup>1,3</sup>, Nan Lu<sup>1</sup>, Fangqun Ouyang<sup>1</sup>, Nan Wang<sup>1</sup>, Guijuan Yang<sup>1</sup>,  
4 Lisheng Kong<sup>2</sup>, Guanzheng Qu<sup>3</sup>, Shougong Zhang<sup>1</sup>, Wenjun Ma<sup>1\*</sup>, and Junhui Wang<sup>1\*</sup>

5 <sup>1</sup>State Key Laboratory of Tree Genetics and Breeding, Key Laboratory of Tree Breeding and  
6 Cultivation of State Forestry Administration, Research Institute of Forestry, Chinese Academy of  
7 Forestry, Beijing 100091, PR China.

8 <sup>2</sup>Department of Biology Centre for Forest Biology, University of Victoria, Victoria 11 BC,  
9 Canada.

10 <sup>3</sup>State Key Laboratory of Tree Genetics and Breeding (Northeast Forestry University), 26 Hexing  
11 Road, Harbin 150040, PR China.

12 **Running title: *SPL* during *C. bungei* flowering**

13 \* To whom correspondence should be addressed. Tel. +086-01062888539.; +086-01062888864.

14 Email: [wangjh808@sina.com](mailto:wangjh808@sina.com) (J.H.W); [mwjlx.163@163.com](mailto:mwjlx.163@163.com) (W.J.M)

## 15 **Abstract**

16 “Bairihua”, a variety of the *Catalpa bungei*, has a large amount of flowers and a long flowering  
17 period which make it an excellent material for flowering researches in trees. SPL is one of the hub  
18 genes that regulate both flowering transition and development. Here, a SPL homologues *CbuSPL9*  
19 was cloned using degenerate primers with RACE. Expression studies during flowering transition  
20 in Bairihua and ectopic expression in *Arabidopsis* showed that *CbuSPL9* was functional similarly  
21 with its *Arabidopsis* homologues. In the next step, we used Y2H to identify the proteins that could  
22 interact with *CbuSPL9*. HMGA, an architectural transcriptional factor, was identified and cloned  
23 for further research. BiFC and BLI showed that *CbuSPL9* could form a heterodimer with  
24 *CbuHMGA* in the nucleus. The expression analysis showed that *CbuHMGA* had a similar  
25 expression trend to that of *CbuSPL9* during flowering in “Bairihua”. Intriguingly, ectopic  
26 expression of *CbuHMGA* in *Arabidopsis* would lead to aberrant flowers, but did not effect  
27 flowering time. Taken together, our results implied a novel pathway that *ChuSPL9* regulated  
28 flowering development, but not flowering transition, with the participation of *ChuHMGA*. Further  
29 investments need to be done to verify the details of this pathway.

30 **Keywords:** *Catalpa bungei*; Flowering; SPL; HMGA; Architectural transcriptional factor.

## 31 **Introduction**

32 Flowers allow flowering plants to have a broader evolutionary relationship and extend their  
33 ecological niche so that they can dominate the terrestrial ecosystem. Flowering is extremely  
34 important for the development of perennial woody plants and for improving the economic value of  
35 plants. However, due to complex genomes and other objective characteristics of perennial woody  
36 plants, research on the flowering process in perennial woody plants remains limited. *Catalpa*  
37 *bungei* is valuable as both a timber and an ornamental tree<sup>1</sup>. “Bairihua”, which is a natural variety  
38 of *C. bungei*, has been characterized for its especially short juvenile period, large number of  
39 flowers and long flowering period. The flowering period of “Bairihua” is approximately 15 days,  
40 and its accumulative flowering period reaches 100 days, which is very rare for woody plants  
41 (<http://www.forestry.gov.cn>). “Bairihua” provides an excellent opportunity to evaluate the  
42 flowering process of woody plants.

43 Flowering is controlled by sophisticated regulatory networks<sup>2-5</sup>. Five major pathways are involved  
44 in these processes, including the aging pathway<sup>6</sup>, gibberellin pathway<sup>7-11</sup>, photoperiod

45 pathway<sup>12–16</sup>, vernalization pathway<sup>17–19</sup> and autonomous pathway<sup>20</sup>. The SQUAMOSA  
46 promoter-binding protein-LIKE (SPL) family of transcription factors (TFs) integrate multiple  
47 pathways<sup>21–25</sup>. *SPLs* have been shown to regulate flowering time and flower organ development in  
48 both herbs and woody plants, such as *Gossypium hirsutum*<sup>26</sup>, maize<sup>27</sup>, birch<sup>28</sup>, *Prunus mume*<sup>29</sup>, and  
49 *Platanus acerifolia*<sup>30</sup>. In the model plant *Arabidopsis*, *AtSPLs* have been shown to be a group of  
50 dominant regulators of the flowering process<sup>4,11,13,22,24,31–34</sup>. The overexpression of *AtSPLs* leads to  
51 early flowering and abnormal inflorescence, and conversely, the inhibition of *AtSPL* expression  
52 delays the occurrence of floral transition<sup>21,35–37</sup>. As a group of TFs, *SPLs* regulate the expression  
53 of other genes. Numerous downstream genes of *SPLs* have been identified; for example, *AtSPL3*  
54 can directly upregulate the expression of *LFY*, *FUL* and *API* by binding to their promoters<sup>38–40</sup>.  
55 However, in addition to protein-DNA interactions, TFs also affect plant growth and development  
56 by forming protein complexes. For example, the MYB-bHLH-WD40/WDR (MBW) complex  
57 regulates late biosynthetic genes in anthocyanin biosynthesis, impacts fruit quality in apple<sup>41,42</sup>,  
58 and regulates trichome initiation in *Arabidopsis thaliana*<sup>43</sup>. Two TFs, AT-HOOK MOTIF  
59 NUCLEAR LOCALIZED PROTEIN 3/4, regulate the formation of the tissue boundary between  
60 the procambium and xylem in *Arabidopsis* roots<sup>44</sup>. Few studies have investigated whether there  
61 are other factors that interact with *SPLs* and affect their binding ability, especially in trees. The  
62 function of *SPLs* in woody plants is still in its infancy.

63 In an effort to study the molecular mechanism of the flowering process in “Bairihua”, we  
64 evaluated whether there were protein interactions involved in *SPL* regulation during the flowering  
65 process. As a first step to address this question, we isolated and characterized the *SPL9*  
66 orthologous gene from “Bairihua” and performed native in planta gene expression analysis. The  
67 putative function of this gene was then tested by ectopic expression experiments. This gene  
68 showed similar expression patterns and the ability to induce flower organ development and early  
69 flowers in *Arabidopsis*. The findings of this study indicated that *CbuSPL9* is functionally  
70 conserved. An architectural TF, *CbuHMGA*, was found via screening *CbuSPL9*-interacting  
71 proteins. *CbuHMGA* is involved in the floral organ development of “Bairihua”, but not in the  
72 regulation of flowering time. These results provide a molecular basis for studying the molecular  
73 mechanism of “Bairihua” flowering and provide a research direction for the study of the floral  
74 transition of perennials.

## 75 **Materials and methods**

### 76 **Plant materials**

77 *C. bungei* is a perennial tree that typically flowers over a 30-day flowering period. However,  
78 “Bairihua”, the new variety of *C. bungei*, was found in Henan Province, China, and confirmed by  
79 the National Forestry and Grassland Administration (<http://www.forestry.gov.cn/>). The flowering  
80 period of a single flower is approximately 15 days, and its accumulative flowering period reaches  
81 100 days, which is very rare for woody plants. From January 15 to April 2, 2017, we collected the  
82 first round of axillary buds of EF and NF varieties every one to two days. Samples were collected  
83 every 10 days during the dormant and germinating periods. Since the floral transition of  
84 “Bairihua” was completed within 7 to 10 days, samples were collected every day during the floral  
85 transition period, and the samples were collected every 5 days during the reproductive growth  
86 stage. The samples used for RNA extraction were washed with distilled water, frozen immediately  
87 in liquid nitrogen, and stored at -80°C. Samples for histological analysis were fixed in a  
88 formalin:glacial acetic acid:70% ethanol (5:5:90 vol.; FAA) solution under a vacuum for at least  
89 24 h.

### 90 **Histological analysis**

91 For histological analysis, the samples were immersed in FAA fixative and placed under vacuum at  
92 4°C. Samples were dehydrated in gradient ethanol and then embedded in paraffin. Ten-mm-thick  
93 sections (RM2255 Fully Automated Rotary Microtome; Leica, Germany) were stained with  
94 Safranin O and fast green FCF (Sigma-Aldrich, USA). The slices were observed and  
95 photographed using a Leica DM 6000B fully automated upright microscope (Leica Microsystems  
96 GmbH, Wetzlar, Germany).

### 97 **Cloning *CbuSPL9* and *CbuHMGA* sequences from “Bairihua”**

98 RNA from “Bairihua” was extracted from the buds of the mutant using an RNA extraction kit  
99 (TaKaRa), and contaminating DNA was removed with RNase-free DNase I (TaKaRa). One or two  
100 micrograms of total mRNA template was added to Oligod (dT)18 primer and reverse-transcribed  
101 into single-stranded cDNA by M-MLV RTase (TaKaRa). The full-length cDNA of *CbuSPL9* was  
102 cloned via 3'-RACE and 5'-RACE by using the (TaKaRa) according to the manufacturer's  
103 instructions. In 3'-RACE, the *CbuSPL9* gene-specific forward primers F1/F2 were designed based  
104 on published and aligned *SPL* sequences from NCBI (<http://blast.ncbi.nlm.nih.gov/Blast.cgi>). F1

105 nested immediately upstream of F2. The 3'-cDNA synthesis primer was provided in a kit. The  
106 PCR products were cloned into the PMD18-T vector and sequenced. *CbuSPL9s* were identified  
107 using BLAST. In 5'-RACE, the gene-specific reverse primers R1/R2 (Supplementary Table S1)  
108 were designed based on sequences from 3'-RACE. R2 nested immediately upstream of R1. The  
109 PCR products were cloned into the PMD18-T vector and sequenced.

#### 110 **Yeast two-hybrid (Y2H) screening of the “Bairihua” cDNA library**

111 A yeast library was constructed by Oebiotech (Shanghai, China) via cloning the full-length cDNA  
112 library from mRNAs in the “Bairihua” buds into the pGADT7 vector<sup>46</sup>. *CbuSPL9* was inserted  
113 into the pGBKT7 vector. Screening of the yeast library was performed using pGBKT7-*CbuSPL9*.  
114 The corresponding primers are listed in Supplementary Table S1. Transformed cells were grown  
115 on SD medium supplemented with Trp. The transformants were screened on supplemented SD  
116 medium lacking Leu, Trp, His and Ade and supplemented with X-a-Gal and Aureobasidin A.  
117 Plates were incubated at 30°C for 48-72 h and photographed. The positive clones were verified  
118 with both pGBKT7 vector consensus primers. Positive control mating was as follows: pGADT7-T  
119 in Y2HGold and pGBK-53 in Y187. Negative control mating was as follows: pGADT7-T in  
120 Y2HGold and pGBKT7-Lam in Y187.

#### 121 **Subcellular localization**

122 To validate subcellular localization, the full-length coding sequences (without the stop codon) of  
123 *CbuSPL9* and *CbuHMGA* were amplified from RNA of “Bairihua” buds by RT-PCR. The PCR  
124 products of *CbuSPL9* and *CbuHMGA* were ligated to the vector pCAMBIA1304 using the  
125 Seamless Assembly Cloning Kit (CloneSmarter, Beijing, China) to construct the  
126 *CbuSPL9/CbuHMGA-GFP* fusion genes driven by a CaMV35S promoter (Niwa, 2003).  
127 pCAMBIA1304-GFP was used as a positive control. The transient expression vectors  
128 *CbuSPL9-GFP*, *CbuHMGA-GFP* and GFP-HDEL were injected into the leaf lower epidermal cells  
129 of *Nicotiana tabacum* L. using *Agrobacterium* transformation as described by Chen et al. (2011).  
130 The transformed cells were incubated for 2 days. The leaves were removed, cut into squares and  
131 immersed in PBS buffer containing 1 g mL<sup>-1</sup> DAPI to stain the nuclei. The transient expression of  
132 the *CbuSPL9/CbuHMGA-GFP* fusion proteins was observed under an UltraVIEW VoX 3D Live  
133 Cell Imaging System Spinning Disk confocal laser scanning microscope (PerkinElmer, Waltham,  
134 MA, USA). The wavelength of excitation used was 488 nm for GFP and 405 nm for DAPI.

### 135 **BiFC analysis**

136 To confirm and visualize the interaction between CbuSPL9 and CbuHMGA in protoplasts from  
137 *Populus trichocarpa*, a BiFC assay was performed based on split EYFP. EYFP was fused to the  
138 C-terminus of CbuSPL9 and the N-terminus of CbuHMGA, resulting in CbuSPL: EYFP<sup>C</sup> and  
139 CbuHMGA: EYFP<sup>N</sup>. A positive EYFP signal indicates an interaction of EYFP<sup>C</sup> and EYFP<sup>N</sup> due to  
140 the heterodimerization of CbuSPL9 with CbuHMGA. CbuSPL: EYFP<sup>C</sup> was cotransfected with  
141 CbuHMGA: EYFP<sup>N</sup> and H2A: mCherry into protoplasts. The transient expression of the  
142 CbuSPL9/CbuHMGA-GFP fusion proteins was observed under an UltraVIEW VoX 3D Live Cell  
143 Imaging System Spinning Disk confocal laser scanning microscope (PerkinElmer, Waltham, MA,  
144 USA).

### 145 **Biolayer interferometry assay**

146 CbuSPL9 was cloned into pGEX6P-1 as a C-terminal GST-tagged construct, and the construct  
147 was confirmed by sequencing. CbuHMGA was cloned into pET28a as an N-terminal 6His-tagged  
148 construct, and the construct was confirmed by sequencing. The protein was purified using the  
149 procedure for EMCV-3C and RV-3C as described above. Real-time interactions between  
150 CbuHMGA and CbuSPL9 were monitored with an Octet QK (Forte-Bio) that is based on BLI<sup>47</sup>.  
151 BLI was used to determine dissociation constants ( $K_D$ ) as well as the on- and off-rate ( $k_{on}$  and  $k_{off}$ )  
152 for HIS-CbuHMG binding to GST-CbuSPL1.

### 153 **Bioinformatic analysis**

154 Multiple sequence alignment and phylogenetic analysis were performed using MEGA6.0. After  
155 alignment, the evolutionary history was calculated using the neighbor-joining (NJ) method. The  
156 tree was inferred from 1000 bootstrap replicates to show the evolutionary history of the genes. The  
157 MEME online tool (<http://meme-suite.org/tools/meme>) was used to identify the motifs of the  
158 CbuSPL9 protein. MEME was run locally with the following parameters: number of repetitions =  
159 any and maximum number of motifs = 20. All candidate interacting protein sequences were  
160 examined by the domain analysis program SMART (Simple Modular Architecture Research Tool)  
161 (<http://smart.embl-heidelberg.de/>).

### 162 **RNA extraction and quantitative real-time PCR**

163 Total RNA was isolated from “Bairihua” buds at different developmental stages. The purity and  
164 quality of RNA was checked by NanoDrop8000 (Thermo Fisher Scientific, Waltham, MA, USA)

165 and analyzed by gel electrophoresis. First-strand cDNA synthesis was carried out with ~1 µg RNA  
166 using the SuperScript III reverse transcription kit (Invitrogen) and random primers according to  
167 the manufacturer's instructions. Primers were designed using Primer 3 online. The melting  
168 temperature of the primers was 60°C, and the amplicon lengths were 100-200 bp. All primers are  
169 listed in Supplementary Table S1. qRT-PCR was performed on a 7500 Real-Time PCR System  
170 (Applied Biosystems, CA, USA) using a SYBR Premix Ex Taq™ Kit (TaKaRa, Dalian, China)  
171 according to the manufacturer's instructions. Relative expression levels were calculated using the  
172 2- $\Delta\Delta C_t$  method. Actin was used as an internal control, and each reaction was conducted in  
173 triplicate. The stem expression values were set to 1.

#### 174 **Transient overexpression in *Arabidopsis thaliana***

175 Full-length CbuSPL9 and CbuHMGA were cloned into the binary vector pBI121 (BD Biosciences  
176 Clontech, USA) under the control of the cauliflower mosaic virus 35S promoter in the sense  
177 orientation. The transgenic plants were generated with the 35S:CbuSPL9 and 35S:CbuHMGA  
178 constructs via *Agrobacterium tumefaciens* GV3101 by using the floral dip method (Clough and  
179 Bent, 1998). Surface-sterilized T1 seeds were grown on a solid 0.5 × MS medium containing 30  
180 µg mL<sup>-1</sup> hygromycin at 4°C for 2 days, which were then transferred to the greenhouse under  
181 long-day conditions (16 h light/8 h dark) at 22°C for 10 days. Subsequently, the seedlings were  
182 transplanted into soil. Phenotypes of the transgenic plants were observed in the T1 generation, and  
183 the overexpression of *CbuSPL9* and *CbuHMGA* in the transgenic plants was confirmed by PCR  
184 genotyping (Supplementary Figure S1 and S2). For each construct, at least 10 transgenic lines  
185 with similar phenotypes were observed, and 3 of them were used for detailed analysis.

#### 186 **Flowering time measurement**

187 Flowering time was measured by counting the total number of rosette leaves and the number of  
188 days to flower (when the floral buds were visible). The numbers of rosette and cauline leaves of  
189 ~20 plants were counted and averaged. The presence of abaxial trichomes was used to  
190 differentiate between the juvenile and adult vegetative leaves. Data were classified with  
191 Win-Excel and analyzed via analysis of variance (ANOVA) using the SPSS (version 8.0, SPSS  
192 Inc., Chicago, IL, USA) statistical package. Comparisons between the treatment means were made  
193 using Tukey's test at a probability level of  $P \leq 0.05$ .

#### 194 **Result**

195 **A flowering-related *SPL* homologous gene was isolated in “Bairihua”**

196 The *SPL* homologous genes in *C. bungei* were isolated by using degenerate primers targeting the  
197 homeodomain. The isolated homeodomain sequences were extended by genome walking to  
198 acquire the full genomic sequences (exons and introns). One of the isolated sequences encoded a  
199 protein with a typical *SPL* protein structure, which included a highly conserved SBP-box domain  
200 bearing two zinc-binding sites and one bipartite nuclear localization signal<sup>45</sup> (Supplementary Table  
201 S2). The first Zn-finger-like structure (ZN-1 in Figure 1a) was C3H-type, and the second (Zn-2 in  
202 Figure 1a) was C2HC-type. The nuclear localization sequence (NLS) is a highly conserved  
203 bipartite domain located at the C-terminus of SBP. Phylogenetic analysis showed that the isolated  
204 sequence clustered with *AtSPL9* and *AtSPL15* (Figure 1b). Since it shared more sequence  
205 similarity with *AtSPL9*, we named the *SPL* homologous gene *CbuSPL9*.

206 **Expression of *CbuSPL9* during the flowering process**

207 Intensive sampling was performed to investigate the changes in *CbuSPL9* expression during the  
208 flowering process (Figure 2). T1-T3 was the dormant period during which no significant  
209 differences in morphology could be observed between the flowering buds (FBs) and the leaf buds  
210 (LBs). T4-T5 was the germination period. During this period, the internal morphology was similar  
211 between the FBs and LBs, but the external morphology of the FBs and LBs had a pale green  
212 appearance compared with that of the FBs and LBs during the dormant period. T6-T9 followed the  
213 short germination period and was the floral transition period, during which flower primordium and  
214 leaf primordium were developed in the FBs and LBs, respectively. Finally, T10-T12 was the  
215 reproductive growth period. The expression level of *CbuSPL9* was significantly higher in the FBs  
216 than in the LBs, especially during the dormant period and the reproductive growth period. Overall,  
217 the expression study supported that *CbuSPL9* was an *SPL* homologous gene and involved in  
218 flowering regulation.

219 **The overexpression of *CbuSPL9* in Arabidopsis**

220 As there is no available transformation system in *C. bungei*, *CbuSPL9* was overexpressed in  
221 Arabidopsis (Columbia ecotype, *col*). The flowers from *col* were tetradynamous and had four  
222 petals distributed in cross type (Figure 3aI). In contrast, the *oe-spl9* transgenic plants showed  
223 aberrant flower organs (Supplementary Table S3). The *oe-spl9* transgenic lines exhibited flower  
224 organs with altered numbers and locations, such as shrunken petals, increased stamens, and



225 overlapping petals (Figure 3aII-VI). In addition to the evident changes in floral organ morphology,  
226 an acceleration in flowering time was observed in the *oe-spl9* lines (Figure 3b, Supplementary  
227 Table S4). The *col* line initiated flowering when 14 rosette leaves were present (Figure 3c).  
228 However, *oe-spl9* possessed less than 9 rosette leaves at the time of bolting (Figure 3d). This result  
229 indicated that the function of *CbuSPL9* was conserved. The regulatory mechanism of *CbuSPL9* in  
230 “Bairihua” might be similar to that in Arabidopsis.

### 231 **Screening *CbuSPL9*-interacting proteins**

232 As a TF, SPL-DNA interaction studies have been extensively performed. However, TFs can also  
233 fine-tune specific biological processes through protein interactions. We constructed a *C. bungei*  
234 yeast two-hybrid cDNA library to explore the proteins that interact with *CbuSPL9*. A total of 809  
235 blue colonies representing potential positive clones were obtained on QDO/Aba/X-a-Gal plates.  
236 The potential positive clones were subsequently tested by PCR for the library plasmid, and 406  
237 clones were positive. The resulting PCR products were sequenced, and the sequences were aligned  
238 using the NCBI BLASTp search function. Finally, 12 interacting protein candidates were  
239 identified (Table 1). These predicted proteins included HMGA, aquaporins, bHLH48,  
240 GATA-related protein, PHD finger protein ALFIN-LIKE 4, heavy metal-associated protein, etc.

### 241 **Cloning the *HMGA* gene**

242 Among these candidates, HMGA, which is an AT-hook rich protein, belongs to the most abundant  
243 nonhistone protein family in the nucleus. We cloned the full-length *HMGA* homologous gene via  
244 rapid amplification of cDNA ends. Phylogenetic analysis revealed that this protein has a close  
245 relationship with AtHMGA. Therefore, this protein was renamed CbuHMGA. *CbuHMGA*  
246 encoded a H15 domain and 4 AT-hook motifs (Figure 4a). The expression analysis showed that the  
247 expression trend of *CbuHMGA* was similar to that of *CbuSPL9* in the four periods in “Bairihua”  
248 (Figure 4b). The expression of *CbuHMGA* was elevated in the dormant period, and the highest  
249 expression level was detected in the reproductive growth period. However, the increase in the  
250 expression of *CbuHMGA* before the reproductive growth period occurred slightly earlier than that  
251 of *CbuSPL9*.

### 252 **Localization of the *CbuSPL9* and *CbuHMGA* proteins**

253 We fused GFP at the C-terminus of *CbuSPL9* and *CbuHMGA* and transformed them into  
254 *Nicotiana benthamiana* leaf epidermal cells to determine the localization of the *CbuSPL9* and

255 CbuHMGA proteins. 35S:GFP was used as a control. The GFP fluorescence in CbuSPL9-GFP and  
256 CbuHMGA-GFP was exclusively observed in the nucleus, whereas the fluorescence of GFP in the  
257 control was distributed throughout the entire cell (Figure 5a). These results showed that CbuSPL9  
258 and CbuHMGA were located in the nucleus. This result was in agreement with the prediction  
259 based on the protein structure.

#### 260 **Protein interaction analysis**

261 Biolayer interferometry (BLI) was used to determine dissociation constants ( $K_D$ ) as well as the on-  
262 and off-rate ( $k_{on}$  and  $k_{off}$ ) for HIS-CbuHMGA binding to GST-CbuSPL9 (Table 2). Five different  
263 concentrations of GST-CbuSPL9 (2381.00 nM, 1191.00 nM, 595.30 nM, 297.60 nM and 148.80 nM)  
264 were evaluated, and the  $K_D$  was 311 nM for each tested concentration. These results suggested a  
265 strong interaction between CbuSPL9 and CbuHMGA (Figure 5b).

266 To confirm these interactions, the full-length cDNA of *CbuSPL9* was inserted into the vector  
267 pGBKT7 (BD-CbuSPL9) as bait, and the full-length cDNA of *CbuHMGA* was inserted into the  
268 vector pGADT7 (AD-CbuHMGA) as prey. Yeast strains containing AD-CbuHMGA and  
269 BD-CbuSPL9 were positive for X- $\alpha$ -gal activity when grown on synthetically defined  
270 (SD)/-Trp/-Leu/-His/-Ade medium (Figure 5c). These results showed that CbuSPL9 interacted  
271 with HMGA in yeast. Finally, a bimolecular fluorescence complementation (BiFC) assay was  
272 performed. CbuSPL9:EYFP<sup>C</sup> was cotransfected with CbuHMGA:EYFP<sup>N</sup> and H2A:mCherry into  
273 protoplasts. The signal of enhanced yellow fluorescent protein (EYFP) was colocalized with  
274 mCherry (Figure 5d). Collectively, we demonstrated that CbuSPL9 formed a heterodimer with  
275 CbuHMGA in the nucleus.

#### 276 **The overexpression of *CbuHMGA* in Arabidopsis**

277 To characterize the potential function of *CbuHMGA*, we overexpressed *CbuHMGA* in Arabidopsis.  
278 The *oe-hmga* transgenic lines developed aberrant flowers with abnormal petals and stamens  
279 (Figure 6aI-VI). This mutant phenotype was similar to the phenotype of floral organs when  
280 *CbuSPL9* was overexpressed (Supplementary Table S5). However, flowering time was not  
281 affected in the *oe-hmga* transgenic lines compared to that in the *col* line (Supplementary Table S6).  
282 The expression of endogenous *AtSPL9* was thoroughly studied to further monitor flower  
283 development in the transgenic lines. Within the sampling period, the expression level of *AtSPL9*  
284 continuously increased in *oe-hmga* and wild type. However, in *oe-spl9*, the expression of *AtSPL9*

285 reached a peak in T6 and then decreased (Figure 6b). The shift in *AtSPL9* expression in *oe-spl9*,  
286 but not in *oe-hmga*, further confirmed the observation that *CbuHMGA* cannot accelerate flower  
287 development, while *CbuSPL9* can accelerate flower development.

## 288 Discussion

289 Flowering is a very complex process, a qualitative change in the life history of higher plants, and a  
290 central link in plant development. “Bairihua”, a variety of the flowering perennial woody plant *C.*  
291 *bungei*, has a large amount of flowers and a long flowering period. “Bairihua” is an excellent  
292 material for evaluating the flowering process in trees.

293 *SPLs* play an important role in regulating flowering in many plants, most notably in Arabidopsis.  
294 In woody plants, *SPLs* are studied extensively, but limited information about flowering is  
295 known<sup>29,48-51</sup>. Here, we cloned the SBP-domain-encoding gene *CbuSPL9* in *C. bungei*. Its  
296 conserved structure and flower development-related expression trends suggest that *CbuSPL9*  
297 might have conserved *SPL9* functions in *C. bungei*. Furthermore, heterogeneous overexpression of  
298 *CbuSPL9* in Arabidopsis accelerated flower development and lead to aberrant flower organs.  
299 Although we could not generate homogenous transgenic plants due to technology and time, these  
300 results are sufficient to demonstrate that *CbuSPL9* is an *SPL* homolog and participates in flower  
301 development.

302 TFs can affect biological processes by forming complexes with other TFs. However, most of the  
303 studies on *SPLs* have focused on their interactions with DNA motifs<sup>38-40</sup>. The proteins that could  
304 directly interact with *SPLs* and participate in flower regulation are largely unknown. For further  
305 insight, we screened the yeast hybridization library for *CbuSPL9* in buds. Many flowering-related  
306 proteins were detected, for example, the GATA-related proteins<sup>52-57</sup>, bHLH48<sup>58</sup>, FLA<sup>59-62</sup>, and  
307 PHD finger protein ALFIN-LIKE<sup>63-65</sup>. Furthermore, a high mobility group (HMG) protein,  
308 *CbuHMGA*, was identified to interact directly with *CbuSPL9*. *CbuHMGA* contains an H15  
309 domain and 4 AT-hook motifs. The BiFC assay and BLI assay further confirmed their interaction.  
310 The BiFC assay suggested that *CbuSPL9* and *CbuHMGA* could form protein complexes in the  
311 nucleus. HMGA proteins have a highly conserved structure<sup>66,67</sup>. Unlike the HMGAs in the animal  
312 kingdom, which invariably contain three AT-hook motifs, most plant HMGA proteins have four  
313 AT-hook motifs<sup>67,68</sup>. Additionally, the amino-terminal region of plant HMGA proteins shares  
314 remarkable homology with the DNA-binding domain of histone H1<sup>69,70</sup>. A similar structural

315 description was confirmed in *CbuHMGA*, which encoded a H15 domain and four AT-hook motifs.  
316 HMGA is an architectural TF<sup>70-73</sup>. It regulates gene expression in vivo by controlling the  
317 formation of multiprotein complexes on the AT-rich regions of certain gene promoters<sup>68,70,81,73-80</sup>.  
318 To date, some plant HMGA proteins have been isolated, such as those in soybean<sup>82</sup>, rice<sup>83</sup>, maize<sup>84</sup>  
319 and *Arabidopsis*<sup>67,73,75,80,85-87</sup>. The *Arabidopsis* HMGA gene was detected in flowers, and  
320 developing siliques had the highest expression<sup>87</sup>. However, studies of the interacting proteins and  
321 the function of HMGA in woody plants are rare. In “Bairihua”, the expression of *CbuHMGA* was  
322 elevated in the dormant period, and the highest expression level was detected in the reproductive  
323 growth period. The result was consistent with that in *Arabidopsis*. Although the *oe-hmga*  
324 transgenic lines did not show a flowering time phenotype, the floral organ mutation of *oe-hmga*  
325 was similar to that of the *oe-spl9* transgenic lines.

326 The HMGA proteins have an important role in biological processes and interact with different  
327 TFs<sup>70,73,88</sup>. Their intrinsic flexibility allows the HMGA proteins to participate in specific  
328 protein-DNA and protein-protein interactions that induce structural changes in chromatin and the  
329 formation of stereospecific complexes called ‘enhanceosomes’ on the promoter/enhancer regions  
330 of genes whose transcription they regulate. The chromatin structure changes affect the ability of  
331 TFs to bind with the promoter/enhancer regions<sup>68,74,77,78,80,85</sup>. From the results in this study, we  
332 suggest that the interaction of *CbuHMGA* with *CbuSPL9* might strengthen or weaken the binding  
333 ability of *CbuSPL9* with the corresponding DNA sequences or downstream proteins, thus  
334 affecting the flowering process. Further experiments are needed to test this hypothesis.

### 335 **Conclusion**

336 “Bairihua” provides us with a valuable opportunity to gain a deeper understanding of the  
337 flowering process of woody plants. Our study showed that *SPLs* may have similar structures and  
338 regulatory mechanisms in perennial trees and *Arabidopsis*. Screening *CbuSPL9*-interacting  
339 proteins revealed not only additional proteins for research on the regulatory pathway of *CbuSPL9*  
340 but also the *CbuSPL9* interaction with *CbuHMGA*. *oe-hmga* showed a phenotype that affected  
341 floral organ development but did not change flowering time. This result suggests that the  
342 mechanism by which *CbuSPL9* affects the flowering process is a complex process, and  
343 *CbuHMGA* is involved in the development of flower organs but not in the regulation of flowering  
344 time.

345 **Conflict of interest**

346 None declared

347 **Funding**

348 This work was supported by Fundamental Research Funds of Chinese Academy of Forestry  
349 (CAFYBB2017ZY002); Fundamental Research Funds of Chinese Academy of Forestry  
350 (CAFYBB2017ZA001-8).

351 **Author contributions**

352 J.H.W., S.G.Z., G.Z.Q., L.I.S., Z.W. and W.J.M. designed the experiments. Z.W. and  
353 W.J.M. analyzed the RNA-seq data and wrote the manuscript. Z.W., and T.Q.Z.  
354 detected the expression of genes using qRT-PCR. Z.W., N.L., F.Q.O.Y., N.W. and  
355 G.J.Y. collected the samples used in the experiment. All the authors have read the  
356 paper and agreed to list their names as co-authors.

357 **Supplementart Data**

358 Supplementary Table S1 The list of the all Primers used in this paper.

359 Supplementary Figure S1 Verification of *oe-SPL9* positive Arabidopsis.

360 Supplementary Figure S2 Verification of *oe-HMGA* positive Arabidopsis.

361 Supplementary Table S2 Details of motif-sequences of CbuSPL9 were identified by MEME.

362 Supplementary Table S3 Statistics of mutant of floral organs in *oe-SPL9* Arabidopsis.

363 Supplementary Table S4 Statistics of mutant of flowering time in *oe-SPL9* Arabidopsis.

364 Supplementary Table S5 Statistics of mutant of floral organs in *oe-HMGA* Arabidopsis.

365 Supplementary Table S6 Statistics of mutant of flowering time in *oe-HMGA* Arabidopsis.

366

367 **References**

- 368 1. Jing, D., Xia, Y., Chen, F., et al. 2015, Ectopic expression of a *Catalpa bungei*  
369 (*Bignoniaceae*) PISTILLATA homologue rescues the petal and stamen identities in  
370 *Arabidopsis pi-1* mutant. *Plant Sci.*, **231**, 40–51.
- 371 2. Flowers, J. M., Hanzawa, Y., Hall, M. C., et al. 2009, Population genomics of the  
372 *Arabidopsis thaliana* flowering time gene network. *Mol. Biol. Evol.*, **26**, 2475–86.
- 373 3. Mouradov, A., Cremer, F., and Coupland, G. 2002, Control of flowering time: interacting  
374 pathways as a basis for diversity. *Plant Cell*, **14 Suppl**, S111–30.
- 375 4. Fornara, F., de Montaigu, A., and Coupland, G. 2010, SnapShot: Control of flowering in  
376 *Arabidopsis*. *Cell*, **141**, 3–5.
- 377 5. Bouché, F., Lobet, G., Tocquin, P., et al. 2016, FLOR-ID: An interactive database of  
378 flowering-time gene networks in *Arabidopsis thaliana*. *Nucleic Acids Res.*, **44**, D1167–71.
- 379 6. Wang, J. 2014, Regulation of flowering time by the miR156-mediated age pathway. *J. Exp.*  
380 *Bot.*, **65**, 4723–7430.
- 381 7. Murase, K., Hirano, Y., Sun, T. P., et al. 2008, Gibberellin-induced DELLA recognition  
382 by the gibberellin receptor GID1. *Nature*, **456**, 459–63.
- 383 8. Eriksson, S. 2006, GA4 Is the Active Gibberellin in the Regulation of LEAFY  
384 Transcription and *Arabidopsis* Floral Initiation. *Plant Cell Online*, **18**, 2172–81.
- 385 9. Livne, S., Lor, V. S., Nir, I., et al. 2015, Uncovering DELLA-Independent Gibberellin  
386 Responses by Characterizing New Tomato *procera* Mutants. *Plant Cell*, **27**, 1579–94.
- 387 10. Cao, D., Cheng, H., Wu, W., et al. 2006, Gibberellin Mobilizes Distinct  
388 DELLA-Dependent Transcriptomes to Regulate Seed Germination and Floral  
389 Development in *Arabidopsis*. *Plant Physiol.*, **142**, 509–25.
- 390 11. Yu, S., Galvao, V. C., Zhang, Y.-C., et al. 2012, Gibberellin Regulates the *Arabidopsis*  
391 Floral Transition through miR156-Targeted SQUAMOSA PROMOTER BINDING-LIKE  
392 Transcription Factors. *Plant Cell*, **24**, 3320–32.
- 393 12. Matsubara, K., Ogiso-tanaka, E., Hori, K., et al. 2017, Natural Variation in Hd17 , a  
394 Homolog of *Arabidopsis* ELF3 That is Involved in Rice Photoperiodic Flowering. *Plant*  
395 *Cell Physiol.*, **53**, 709–16.
- 396 13. Jung, J. H., Ju, Y., Seo, P. J., et al. 2012, The SOC1-SPL module integrates photoperiod

- 397 and gibberellic acid signals to control flowering time in Arabidopsis. *Plant J.*, **69**, 577–88.
- 398 14. Minmin, S., and Youjun, H. 2018, Advances of GIGANTEA and CONSTANS, the Key  
399 Genes of Flowering in Photoperiod Pathway. *Mol. Plant Breed.*, **16**, 5601–7.
- 400 15. Wang, H., Pan, J., Li, Y., et al. 2016, The DELLA-CONSTANS Transcription Factor  
401 Cascade Integrates Gibberellic Acid and Photoperiod Signaling to Regulate Flowering.  
402 *Plant Physiol.*, **172**, 479–88.
- 403 16. Cano, B., Ruiz, M. T., Romero, J. M., et al. 2014, Photoperiodic Control of Carbon  
404 Distribution during the Floral Transition in Arabidopsis. *Plant Cell*, **26**, 565–84.
- 405 17. Huang, B., Qian, P., Gao, N., et al. 2017, Fackel interacts with gibberellic acid signaling  
406 and vernalization to mediate flowering in Arabidopsis. *Planta*, **245**, 939–50.
- 407 18. Kim, D.-H., and Sung, S. 2013, Coordination of the Vernalization Response through a  
408 VIN3 and FLC Gene Family Regulatory Network in Arabidopsis. *Plant Cell*, **25**, 454–69.
- 409 19. Heo, J. B., and Sung, S. 2011, Vernalization-mediated epigenetic silencing by a long  
410 intronic noncoding RNA. *Science (80-. )*, **331**, 76.
- 411 20. Simpson, G. G. 2004, The autonomous pathway: Epigenetic and post-transcriptional gene  
412 regulation in the control of Arabidopsis flowering time. *Curr. Opin. Plant Biol.*, **7**, 570–4.
- 413 21. Unte, U. S. 2003, SPL8, an SBP-Box Gene That Affects Pollen Sac Development in  
414 Arabidopsis. *Plant Cell Online*, **15**, 1009–19.
- 415 22. Yu, N., Niu, Q. W., Ng, K. H., et al. 2015, The role of miR156/SPLs modules in  
416 Arabidopsis lateral root development. *Plant J.*, **83**, 673–85.
- 417 23. Casero, D., Singh, V., Wilson, G. T., et al. 2012, Transcriptome Sequencing Identifies  
418 SPL7-Regulated Copper Acquisition Genes FRO4/FRO5 and the Copper Dependence of  
419 Iron Homeostasis in Arabidopsis. *Plant Cell Online*, **24**, 738–61.
- 420 24. Jung, J. H., Lee, H. J., Ryu, J. Y., et al. 2016, SPL3/4/5 Integrate Developmental Aging  
421 and Photoperiodic Signals into the FT-FD Module in Arabidopsis Flowering. *Mol. Plant*, **9**,  
422 1647–59.
- 423 25. Preston, J. C., and Hileman, L. C. 2013, Functional Evolution in the Plant  
424 SQUAMOSA-PROMOTER BINDING PROTEIN-LIKE (SPL) Gene Family. *Front. Plant*  
425 *Sci.*, **4**, 1–13.
- 426 26. Zhang, X., Dou, L., Pang, C., et al. 2015, Genomic organization , differential expression ,

- 427 and functional analysis of the SPL gene family in *Gossypium hirsutum*. *Mol. Genet.*  
428 *Genomics*, **290**, 115–26.
- 429 27. Mao, H. De, Yu, L. J., Li, Z. J., et al. 2016, Genome-wide analysis of the SPL family  
430 transcription factors and their responses to abiotic stresses in maize. *Plant Gene*, **6**, 1–12.
- 431 28. Lannenpaa, M., Janonen, I., Sopanen, T., et al. 2004, A new SBP-box gene BpSPL1 in  
432 silver birch (*Betula pendula*). *Physiol. Plant.*, **120**, 491–500.
- 433 29. Xu, Z., Sun, L., Zhou, Y., et al. 2015, Identification and expression analysis of the  
434 SQUAMOSA promoter-binding protein (SBP)-box gene family in *Prunus mume*. *Mol.*  
435 *Genet. Genomics*, **290**, 1701–15.
- 436 30. Han, H., Liu, G., Zhang, J., et al. 2016, Four SQUAMOSA PROMOTER BINDING  
437 PROTEIN-LIKE homologs from a basal eudicot tree (*Platanus acerifolia*) show diverse  
438 expression pattern and ability of inducing early flowering in *Arabidopsis*. *Trees*, **30**,  
439 1417–28.
- 440 31. Xing, S., Salinas, M., Höhmann, S., et al. 2010, miR156-Targeted and Nontargeted  
441 SBP-Box Transcription Factors Act in Concert to Secure Male Fertility in *Arabidopsis* .  
442 *Plant Cell*, **22**, 3935–50.
- 443 32. Yamasaki, H., Hayashi, M., Fukazawa, M., et al. 2009, SQUAMOSA Promoter Binding  
444 Protein-Like7 Is a Central Regulator for Copper Homeostasis in *Arabidopsis*. *Plant Cell*  
445 *Online*, **21**, 347–61.
- 446 33. Xing, S., Salinas, M., Garcia-Molina, A., et al. 2013, SPL8 and miR156-targeted SPL  
447 genes redundantly regulate *Arabidopsis* gynoecium differential patterning. *Plant J.*, **75**,  
448 566–77.
- 449 34. Yan, J., Chia, J.-C., Sheng, H., et al. 2017, *Arabidopsis* Pollen Fertility Requires the  
450 Transcription Factors CIT1 and SPL7 that Regulate Copper Delivery to Anthers and  
451 Jasmonic Acid Synthesis. *Plant Cell*, tpc.00363.2017.
- 452 35. Poethig, R. S. 2013, Vegetative phase change and shoot maturation in plants. *Curr. Top.*  
453 *Dev. Biol.*, **105**, 125–52.
- 454 36. Yu, N., Cai, W.-J., Wang, S., et al. 2010, Temporal Control of Trichome Distribution by  
455 MicroRNA156-Targeted SPL Genes in *Arabidopsis thaliana*. *Plant Cell Online*, **22**,  
456 2322–35.



- 457 37. Hyun, Y., Richter, R., and Coupland, G. 2016, Competence to Flower: Age-Controlled  
458 Sensitivity to Environmental Cues. *Plant Physiol.*, **173**, 36–46.
- 459 38. Wu, G. 2006, Temporal regulation of shoot development in *Arabidopsis thaliana* by  
460 miR156 and its target SPL3. *Development*, **133**, 3539–47.
- 461 39. Yamaguchi, A., Wu, M. F., Yang, L., et al. 2009, The MicroRNA-Regulated SBP-Box  
462 Transcription Factor SPL3 Is a Direct Upstream Activator of LEAFY, FRUITFULL, and  
463 APETALA1. *Dev. Cell*, **17**, 268–78.
- 464 40. Wang, J. W., Czech, B., and Weigel, D. 2009, miR156-Regulated SPL Transcription  
465 Factors Define an Endogenous Flowering Pathway in *Arabidopsis thaliana*. *Cell*, **138**,  
466 738–49.
- 467 41. An, X. H., Tian, Y., Chen, K. Q., et al. 2015, MdMYB9 and MdMYB11 are involved in  
468 the regulation of the ja-induced biosynthesis of anthocyanin and proanthocyanidin in  
469 apples. *Plant Cell Physiol.*, **56**, 650–62.
- 470 42. Xie, X. Bin, Li, S., Zhang, R. F., et al. 2012, The bHLH transcription factor MdbHLH3  
471 promotes anthocyanin accumulation and fruit colouration in response to low temperature  
472 in apples. *Plant, Cell Environ.*, **35**, 1884–97.
- 473 43. Qi, T., Song, S., Ren, Q., et al. 2011, The Jasmonate-ZIM-Domain Proteins Interact with  
474 the WD-Repeat/bHLH/MYB Complexes to Regulate Jasmonate-Mediated Anthocyanin  
475 Accumulation and Trichome Initiation in *Arabidopsis thaliana*. *Plant Cell*, **23**, 1795–814.
- 476 44. Zhou, J., Wang, X., Lee, J.-Y. 2013, Cell-to-Cell Movement of Two Interacting AT-Hook  
477 Factors in *Arabidopsis* Root Vascular Tissue Patterning. *Plant Cell*, **25**, 187–201.
- 478 45. Kropat, J., Tottey, S., Birkenbihl, R. P., et al. 2005, A regulator of nutritional copper  
479 signaling in *Chlamydomonas* is an SBP domain protein that recognizes the GTAC core of  
480 copper response element. *Proc. Natl. Acad. Sci.*, **102**, 18730–5.
- 481 46. Yan, T., Chen, M., Shen, Q., et al. 2017, HOMEODOMAIN PROTEIN 1 is required for  
482 jasmonate-mediated glandular trichome initiation in *Artemisia annua*. *New Phytol.*, **213**,  
483 1145–55.
- 484 47. Zhang, Y., Mao, D., Roswit, W. T., et al. 2015, PARP9-DTX3L ubiquitin ligase targets  
485 host histone H2BJ and viral 3C protease to enhance interferon signaling and control viral  
486 infection. *Nat. Immunol.*, **16**, 1215–27.

- 487 48. Castillo, M. C., Forment, J., Gadea, J., et al. 2013, Identification of transcription factors  
488 potentially involved in the juvenile to adult phase transition in Citrus. *Ann. Bot.*, **112**,  
489 1371–81.
- 490 49. Tewari, S., and Buonaccorsi, J. P. 2013, Impact of Early Season Apical Meristem Injury  
491 by Gall Inducing Tipworm (Diptera: Cecidomyiidae) on Reproductive and Vegetative  
492 Growth of Cranberry Entomology. *J. Econ. Entomol.*, **106**, 1339–48.
- 493 50. Lannenpaa, M., Janonen, I., Sopanen, T., et al. 2004, A new SBP-box gene BpSPL1 in  
494 silver birch (*Betula pendula*). *Physiol. Plant.*, **120**, 491–500.
- 495 51. Lu, C. L. and S. 2014, Molecular characterization of the SPL gene family in *Populus*  
496 *trichocarpa*. *BMC Plant Biol.*, **14**, 131.
- 497 52. Zhang, X., Zhou, Y., Ding, L., et al. 2013, Transcription Repressor HANABA TARANU  
498 Controls Flower Development by Integrating the Actions of Multiple Hormones, Floral  
499 Organ Specification Genes, and GATA3 Family Genes in Arabidopsis. *Plant Cell*, **25**,  
500 83–101.
- 501 53. Ding, L., Yan, S., Jiang, L., et al. 2015, HANABA TARANU (HAN) Bridges Meristem  
502 and Organ Primordia Boundaries through PINHEAD, JAGGED, BLADE-ON-PETIOLE2  
503 and CYTOKININ OXIDASE 3 during Flower Development in Arabidopsis. *PLoS Genet.*,  
504 **11**, 1–23.
- 505 54. Ding, L., Yan, S., Jiang, L., et al. 2015, HANABA TARANU regulates the shoot apical  
506 meristem and leaf development in cucumber (*Cucumis sativus* L.). *J. Exp. Bot.*, **66**,  
507 7075–87.
- 508 55. Mara, C. D., and Irish, V. F. 2008, Two GATA Transcription Factors Are Downstream  
509 Effectors of Floral Homeotic Gene Action in Arabidopsis. *Plant Physiol.*, **147**, 707–18.
- 510 56. Richter, R., Bastakis, E., and Schwechheimer, C. 2013, Cross-Repressive Interactions  
511 between SOC1 and the GATAs GNC and GNL/CGA1 in the Control of Greening, Cold  
512 Tolerance, and Flowering Time in Arabidopsis. *Plant Physiol.*, **162**, 1992–2004.
- 513 57. Wang, L., Yin, H., Qian, Q., et al. 2009, NECK LEAF 1, a GATA type transcription factor,  
514 modulates organogenesis by regulating the expression of multiple regulatory genes during  
515 reproductive development in rice. *Cell Res.*, **19**, 598–611.
- 516 58. Li, Y., Wang, H., Li, X., et al. 2017, Two DELLA-interacting proteins bHLH48 and

- 517 bHLH60 regulate flowering under long-day conditions in *Arabidopsis thaliana*. *J. Exp.*  
518 *Bot.*, **68**, 2757–67.
- 519 59. Li, J., Yu, M., Geng, L. L., et al. 2010, The fasciclin-like arabinogalactan protein gene,  
520 FLA3, is involved in microspore development of *Arabidopsis*. *Plant J.*, **64**, 482–97.
- 521 60. Johnson, K. L. 2003, The Fasciclin-Like Arabinogalactan Proteins of *Arabidopsis*. A  
522 Multigene Family of Putative Cell Adhesion Molecules. *Plant Physiol.*, **133**, 1911–25.
- 523 61. Johnson, K. L., Kibble, N. A. J., Bacic, A., et al. 2011, A fasciclin-like  
524 Arabinogalactan-protein (FLA) mutant of *Arabidopsis thaliana*, *fla1*, shows defects in  
525 shoot regeneration. *PLoS One*, **6**, 1–11.
- 526 62. Zhang, Z., Wang, C., Kong, F., et al. 2017, Fasciclin-like arabinogalactan proteins,  
527 PtFLAs, play important roles in GA-mediated tension wood formation in *Populus*. *Sci.*  
528 *Rep.*, **7**, 1–13.
- 529 63. Shu, K., Chen, Q., Wu, Y., et al. 2016, ABSCISIC ACID-INSENSITIVE 4 negatively  
530 regulates flowering through directly promoting *Arabidopsis* FLOWERING LOCUS C  
531 transcription. *J. Exp. Bot.*, **67**, 195–205.
- 532 64. Song, Y., Gao, J., Yang, F., et al. 2013, Molecular Evolutionary Analysis of the  
533 Alfin-Like Protein Family in *Arabidopsis lyrata*, *Arabidopsis thaliana*, and *Thellungiella*  
534 *halophila*. *PLoS One*, **8**, e66838.
- 535 65. Pan, W.-J., Zhang, J.-S., Tao, J.-J., et al. 2018, An Alfin-like gene from *Atriplex hortensis*  
536 enhances salt and drought tolerance and abscisic acid response in transgenic *Arabidopsis*.  
537 *Sci. Rep.*, **8**, 1–13.
- 538 66. Grasser, K. D. 2003, Chromatin-associated HMGA and HMGB proteins: Versatile  
539 co-regulators of DNA-dependent processes. *Plant Mol. Biol.*, **53**, 281–95.
- 540 67. Klosterman, S. J., and Hadwiger, L. A. 2002, Plant HMG proteins bearing the AT-hook  
541 motif. *Plant Sci.*, **162**, 855–66.
- 542 68. Dragan, A. I., Liggins, J. R., Crane-Robinson, C., et al. 2003, The energetics of specific  
543 binding of AT-hooks from HMGA1 to target DNA. *J. Mol. Biol.*, **327**, 393–411.
- 544 69. Krech, A. B., Wulff, D., Grasser, K. D., et al. 1999, Plant chromosomal HMGI/Y proteins  
545 and histone H1 exhibit a protein domain of common origin. *Gene*, **230**, 1–5.
- 546 70. Reeves, R. 2001, Molecular biology of HMGA proteins : hubs of nuclear function. *Gene*,

- 547           **277**, 63–81.
- 548   71.   Tessari, M. A., Gostissa, M., Altamura, S., et al. 2003, Transcriptional Activation of the  
549           Cyclin A Gene by the Architectural Transcription Factor HMGA2. *Mol. Cell. Biol.*, **23**,  
550           9104–16.
- 551   72.   Reeves, R., and Beckerbauer, L. 2001, HMGI/Y proteins:flexible regulators of transcription  
552           and chromatin structure. *BBA-Biochimica Biophys. Acta*, **1519**, 13–29.
- 553   73.   Sgarra, R., Zammitti, S., Lo Sardo, A., et al. 2010, HMGA molecular network: From  
554           transcriptional regulation to chromatin remodeling. *Biochim. Biophys. Acta - Gene Regul.*  
555           *Mech.*, **1799**, 37–47.
- 556   74.   Gonzalez, N., Pauwels, L., Baekelandt, A., et al. 2015, A Repressor Protein Complex  
557           Regulates Leaf Growth in Arabidopsis. *Plant Cell*, **27**, 2273–87.
- 558   75.   Rodríguez-concepción, M., and Rodri, M. 1999, Arachidonic Acid Alters Tomato HMG  
559           Expression and Fruit Growth and Induces 3- Hydroxy-3-Methylglutaryl Coenzyme. *Plant*  
560           *Physiol.*, **119**, 41–8.
- 561   76.   Reeves, R., and Beckerbauer, L. 2001, HMGI/Y proteins: Flexible regulators of  
562           transcription and chromatin structure. *Biochim. Biophys. Acta - Gene Struct. Expr.*, **1519**,  
563           13–29.
- 564   77.   Richter, T., Mu, T. E., Heinkele, G., et al. 2005, Interaction between HMGA1a and the  
565           origin recognition complex creates site-specific replication origins. *PNAS*, **308**, 1–24.
- 566   78.   Norseen, J., Thomae, A., Sridharan, V., et al. 2008, RNA-dependent recruitment of the  
567           origin recognition complex. *EMBO J.*, **27**, 3024–35.
- 568   79.   Gupta, R., Webster, C. I., and Gray, J. C. 1997, The single-copy gene encoding  
569           high-mobility-group protein HMG-I/Y from pea contains a single intron and is expressed  
570           in all organs. *Plant Mol. Biol.*, **35**, 987–92.
- 571   80.   Matsushita, A., Furumoto, T., Ishida, S., et al. 2007, AGF1, an AT-Hook Protein, Is  
572           Necessary for the Negative Feedback of AtGA3ox1 Encoding GA 3-Oxidase. *Plant*  
573           *Physiol.*, **143**, 1152–62.
- 574   81.   Reeves, R., and Beckerbauer, L. 2001, HMGI/Y proteins: Flexible regulators of  
575           transcription and chromatin structure. *Biochim. Biophys. Acta - Gene Struct. Expr.*, **1519**,  
576           13–29.

- 577 82. Laux, T., Seurinck, J., and Goldberg, R. B. 1991, A soybean embryo cDNA encodes a  
578 DNA binding protein with histone and HMG-protein-like domains. *Nucleic Acids Res.*, **19**,  
579 4768.
- 580 83. Yamamoto, S., and Minamikawa, T. 1997, Two genes for the high mobility group protein  
581 HMG-Y are present in the genome of *Canavalia gladiata* D.C. *Plant Mol. Biol.*, **33**,  
582 537–44.
- 583 84. Zhao, J., Paul, L. K., and Grafi, G. 2009, The maize HMGA protein is localized to the  
584 nucleolus and can be acetylated in vitro at its globular domain, and phosphorylation by  
585 CDK reduces its binding activity to AT-rich DNA. *Biochim. Biophys. Acta - Gene Regul.*  
586 *Mech.*, **1789**, 751–7.
- 587 85. Pierantoni, G. M., Rinaldo, C., Esposito, F., et al. 2006, High Mobility Group A1  
588 (HMGA1) proteins interact with p53 and inhibit its apoptotic activity. *Cell Death Differ.*,  
589 **13**, 1554–63.
- 590 86. Cho, J. H., Kim, M. J., Kim, K. J., et al. 2011, POZ / BTB and AT-hook-containing zinc  
591 finger protein 1 ( PATZ1 ) inhibits endothelial cell senescence through a p53 dependent  
592 pathway. *Cell Death Differ.*, **19**, 703–12.
- 593 87. Xiao, C., Chen, F., Yu, X., et al. 2009, Over-expression of an AT-hook gene, AHL22,  
594 delays flowering and inhibits the elongation of the hypocotyl in *Arabidopsis thaliana*.  
595 *Plant Mol. Biol.*, **71**, 39–50.
- 596 88. Michela A. T., Monica Gostissa, Sandro Altamura, et al. 2004, Transcriptional Activation  
597 of the Cyclin A Gene by the Architectural Transcription Factor HMGA2. *Mol. Cell. Biol.*,  
598 **23**, 9104–16.
- 599

600 **Table 1 Details of the proteins interacting with the CbuSPL9 protein**

Annotation	Quantity
Sesamum indicum HMG-Y-related protein B-like (LOC105159884), mRNA	4
PREDICTED: Sesamum indicum aquaporin PIP2-4-like (LOC105174310), mRNA	1
PREDICTED: Sesamum indicum GATA transcription factor 8 (LOC105166606), transcript variant X2, mRNA	1
PREDICTED: Sesamum indicum heavy metal-associated isoprenylated plant protein 33-like (LOC105156967), mRNA	2
PREDICTED: Sesamum indicum probable E3 ubiquitin ligase SUD1 (LOC105169523), mRNA	4
PREDICTED: Erythranthe guttatus transcription factor bHLH148-like (LOC105966580), mRNA	1
PREDICTED: Sesamum indicum aquaporin TIP1-1-like (LOC105170758), mRNA	1
PREDICTED: Sesamum indicum probable GTP diphosphokinase RSH2, chloroplastic (LOC105157806), transcript variant X1, mRNA	1
Arabidopsis thaliana proline-rich family protein mRNA ( PRPs )	1
PREDICTED: Sesamum indicum fasciclin-like arabinogalactan protein 17 (LOC105161692), mRNA	1
PREDICTED: Erythranthe guttatus MAG2-interacting protein 2 (LOC105963338), mRNA	1

601

602 **Table 2 Interaction between HIS-CbuHMGA and GST-CbuSPL9 by BLI**

Protein1	Protein2	Conc. of Protein2/nM	$K_{on}/Ms$	$K_{off}/s$	$K_D/nM$
HIS-CbuHMGA	GST-CbuSPL9	2381	5.40E-04	1.74E+03	311
HIS-CbuHMGA	GST-CbuSPL9	1191	5.40E-04	1.74E+03	311
HIS-CbuHMGA	GST-CbuSPL9	595.3	5.40E-04	1.74E+03	311
HIS-CbuHMGA	GST-CbuSPL9	297.6	5.40E-04	1.74E+03	311
HIS-CbuHMGA	GST-CbuSPL9	148.8	5.40E-04	1.74E+03	311

603

604 **Figure 1 The phylogenetic relationship and motif composition analysis of the CbuSPL9 gene**  
605 **in *C. bungei*.** a) Multiple sequence alignment and sequence logo of the *C. bungei* SBP-box  
606 domain. Sequence alignment was performed with DNAMAN. The two conserved zinc fingers and  
607 NLS are indicated. The sequence logo was obtained from MEME online software. The overall  
608 height of the stack indicates the sequence conservation at that position. b) The phylogenetic tree  
609 was constructed with MEGA 6.0 by the neighbor-joining (NJ) method with 1000 bootstrap  
610 replicates. Bootstrap support is indicated at each node. *A. thaliana* (At), *C. bungei* (Cbu).

611 **Figure 2 Expression profile of *CbuSPL9* in the flower buds and leaf buds during the**  
612 **developmental periods of *C. bungei*.** T1-T3 represents the flowering buds and leaf buds collected  
613 in the dormant period; T4-T5 represents the flowering buds and leaf buds collected in the  
614 germination period; T6-T9 represents the flowering buds and leaf buds collected in the floral  
615 transition period; and T10-T12 represents the flowering buds and leaf buds collected in the  
616 reproductive period. D1: Image of flowering buds in the dormant period; D2: Image of leaf buds  
617 in the dormant period; G1: Image of flowering buds in the germination period; G2: Image of leaf  
618 buds in the germination period; F1: Section of flowering buds in the floral transition period; note  
619 the flat generative apex (Ga); F2: Section of leaf buds in floral transition period, note the bulged  
620 vegetative apex (V); R1: Image of flowering buds in the reproductive period; and R2: Image of  
621 leaf buds in the reproductive period. Notably, even though floral transition was never observed in  
622 the leaf buds, the leaf buds collected in the period corresponding to floral transition are henceforth  
623 called F2 and R2 for convenience. Error bars indicate SD from three independent biological  
624 replicates. \*Difference between flowering buds (black) and leaf buds (gray) is significant  
625 (Student's test;  $p < 0.05$ ). \*\*Difference between flowering buds (black) and leaf buds (gray) is  
626 highly significant (Student's test;  $p < 0.01$ ).

627 **Figure 3 Phenotype of overexpression mutants of *CbuSPL9*.** a) The change in floral organs  
628 occurred in the *CbuSPL9*-overexpressing transgenic *Arabidopsis* lines. Image of a normal flower  
629 from col as the control (a/I); and the floral organ mutant from *oespl9* (a/II-VI). b) Comparison of  
630 the flowering phenotype in both the col and *oespl9* transgenic plants. From top to bottom: col  
631 (control) and *oespl9* (transgenic plants). c) and d) are the statistical data of the time of flower bud  
632 emergence and the number of rosette leaves. The *oespl9* transgenic plants (black), the *oe-hmga*  
633 transgenic plants (gray) and the col plants (white). A total of 30 plants were averaged to obtain the






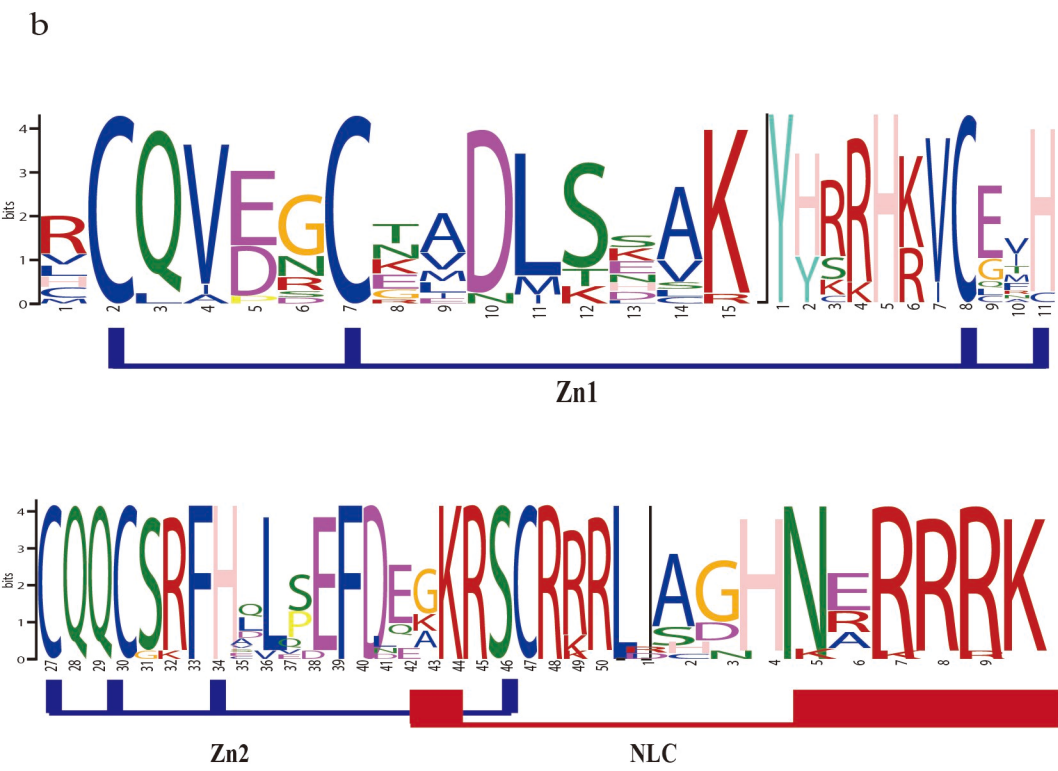
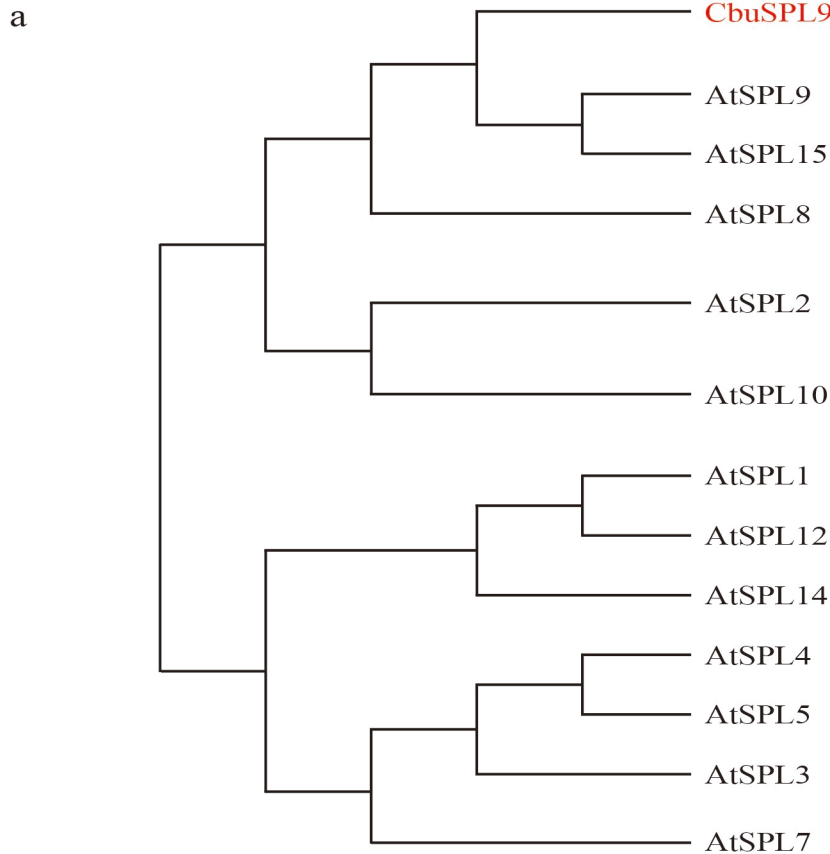
634 mean. Error bars indicate SD.

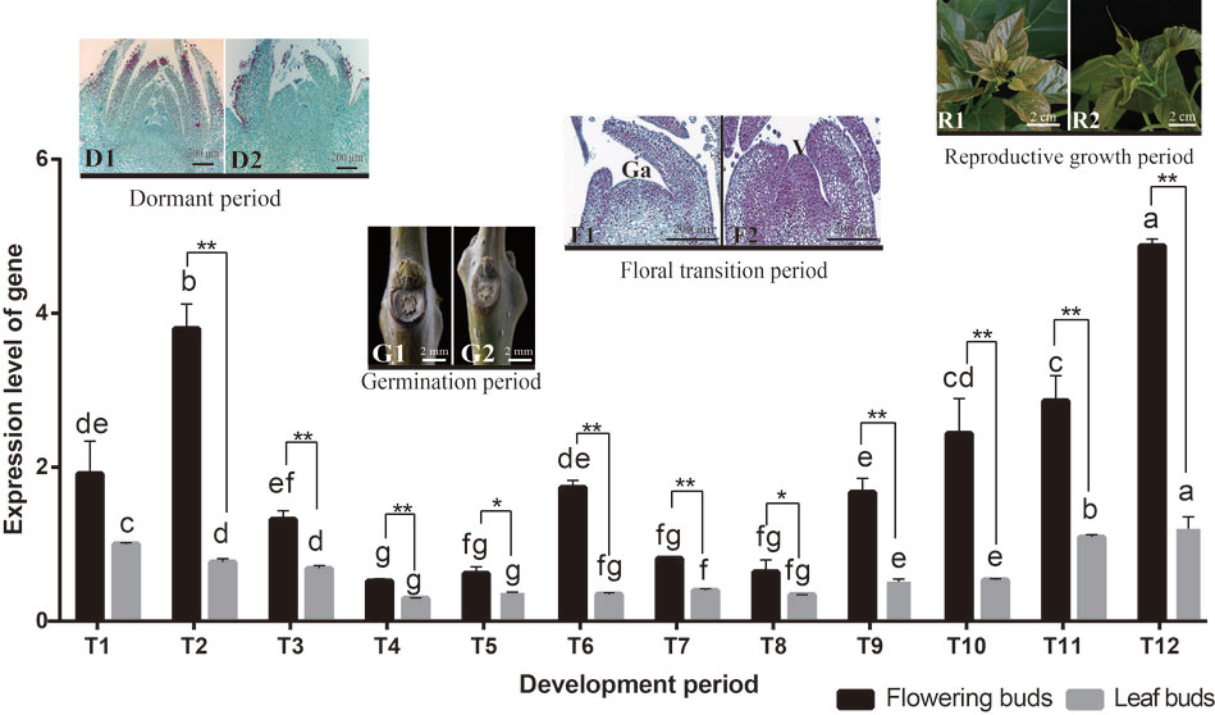
635 **Figure 4 The sequence and expression profile analysis of *CbuHMGA*.** a) Sequence analysis of  
636 the *CbuHMGA* protein by SMART. b) The expression analysis of *CbuHMGA* between flowering  
637 buds and leaf buds during the development periods. T1-T3 represents the flowering buds and leaf  
638 buds collected in the dormant period; T4-T5 represents the flowering buds and leaf buds collected  
639 in the germination period; T6-T9 represents the flowering buds and leaf buds collected in the  
640 floral transition period; and T10-T12 represents the flowering buds and leaf buds collected in the  
641 reproductive period. Notably, even though floral transition was never observed in the leaf buds,  
642 the leaf buds collected in the period corresponding to floral transition are henceforth called the  
643 floral transition period and reproductive period for convenience. Error bars indicate SD from three  
644 independent experiments. \*Difference between flowering buds (black) and leaf buds (gray) is  
645 significant (Student's test;  $p < 0.05$ ). \*\*Difference between flowering buds (black) and leaf buds  
646 (gray) is highly significant (Student's test;  $p < 0.01$ ).

647 **Figure 5 Interaction between the two proteins *CbuSPL9* and *CbuHMGA*.** a) Nuclear  
648 localization of the *CbuSPL9* protein and *CbuHMGA* protein. The GFP (control) gene,  
649 *CbuSPL9*-GFP fusion gene and *CbuHMGA*-GFP fusion gene were expressed transiently in  
650 *Nicotiana benthamiana* leaf epidermal cells and observed with confocal microscopy. DAPI, DAPI  
651 for nuclear staining image; GFP, GFP green fluorescence image; Merge, the merged images of  
652 bright-field, GFP and DAPI staining. b) Binding of GST-*CbuSPL9* to HIS-*CbuHMGA*, with  
653 GST-*CbuSPL9* concentrations of 2381.00 nm, 1191.0 nm, 595.30 nm, 297.60 nm, 148.80 nm  
654 assessed by real-time biolayer interferometry. c) Yeast two-hybrid assays for the interactions  
655 between *CbuSPL9* and *CbuHMGA*. *CbuHMGA* (as prey) was fused with the GAL4 activation  
656 domain (AD) in pGADT7, while *CbuSPL9* (as bait) was fused with the GAL DNA-binding  
657 domain (BD) in pGBKT7. The positive control was as follows: pGADT7-T and pGBK-53. The  
658 negative control was as follows: pGADT7-T and pGBK-Lam. Interactions are indicated by the  
659 blue color on SD/-Trp/-Leu/-His/-Ade/X- $\alpha$ -gal medium. d) Confocal images of the BiFC analysis  
660 in protoplasts from *P. trichocarpa*. *CbuSPL9* was fused with EYFP<sup>C</sup>, and *CbuHMGA* was fused  
661 with EYFP<sup>N</sup>. EYFP signal was detected in the nucleus of the S1-21 protoplasts transfected by  
662 H2A:mCherry and *CbuSPL9*:EYFP<sup>C</sup> with (A) *CbuHMGA*:EYFP<sup>N</sup>. Bars=50  $\mu$ m.

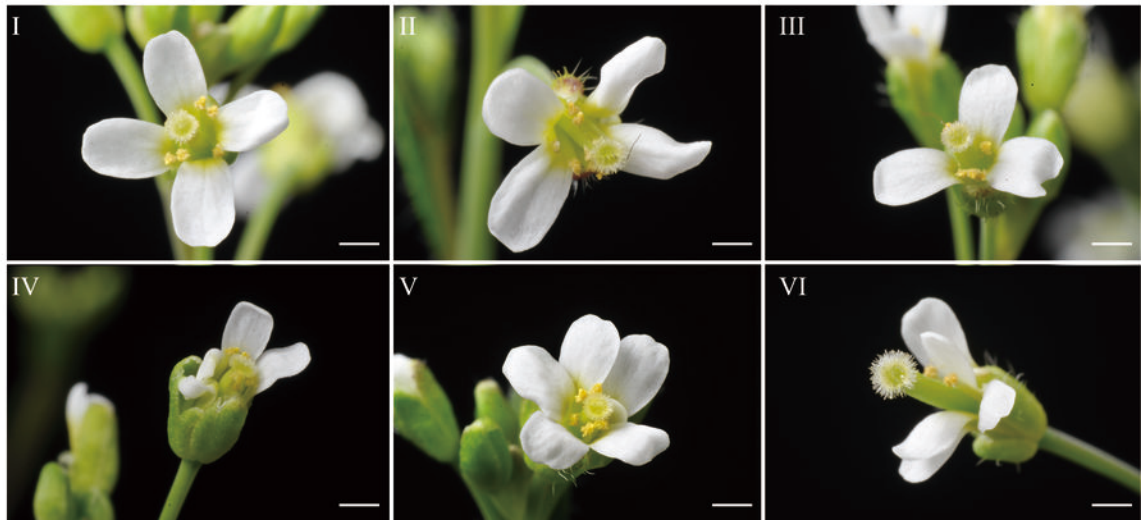
663 **Figure 6 Phenotype of overexpression mutants of *CbuHMGA*.** a) The change in floral organs

664 occurred in the overexpression of the CbuHMGA transgenic Arabidopsis lines. The images are the  
665 floral organ mutant from oe-hmga transgenic Arabidopsis lines (a/I-VI). b) Expression profiles of  
666 atSPL9 homologous genes in the oespl9 transgenic plants, oe-hmga transgenic plants and col.  
667  represents the PCR results in oe-hmga;  represents the PCR results in oespl9; and   
668 represents the PCR results in col. Three independent biological replicates were performed, and  
669 each replicate was measured in triplicate. The error bars show the standard deviation of the results  
670 of three technical replicates.

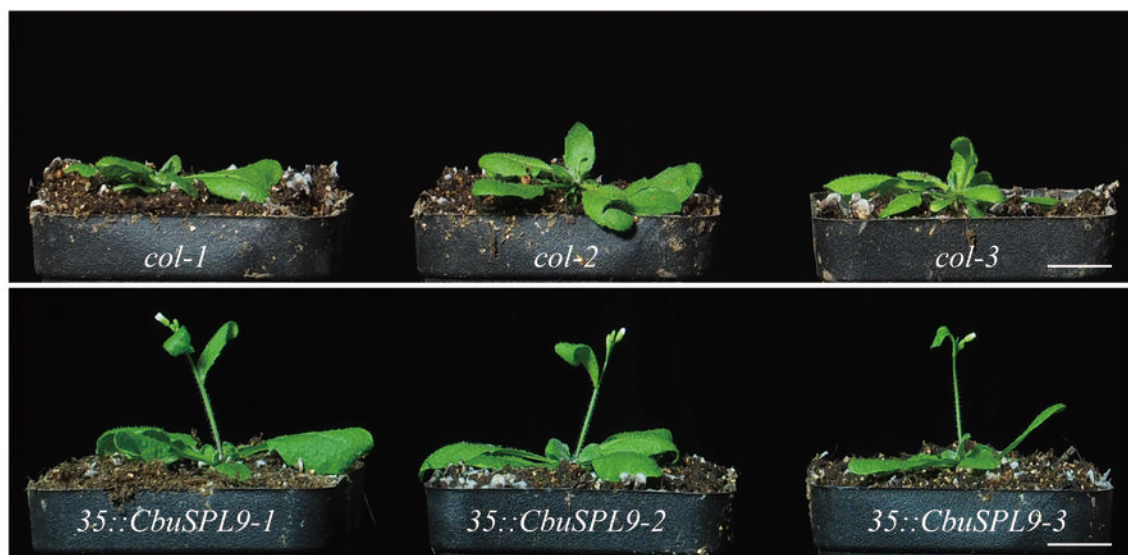




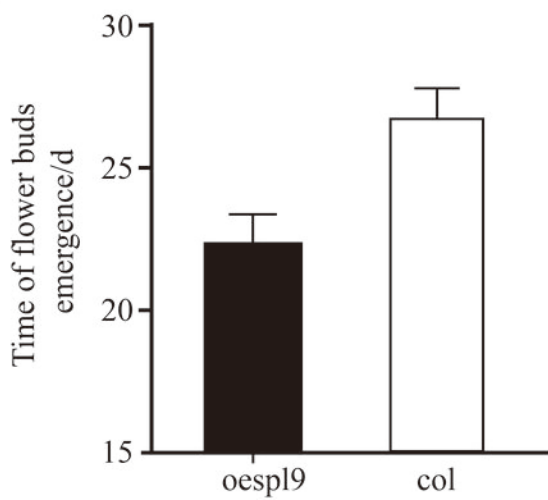
a



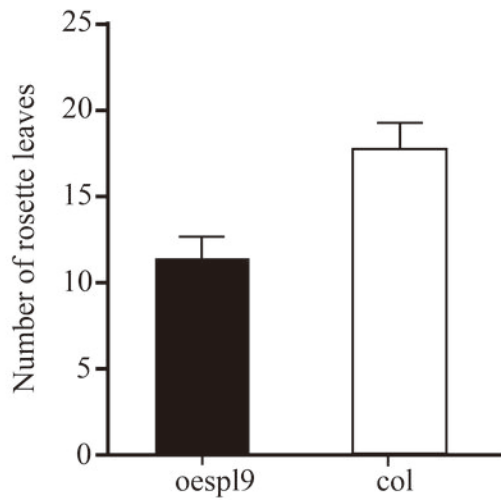
b



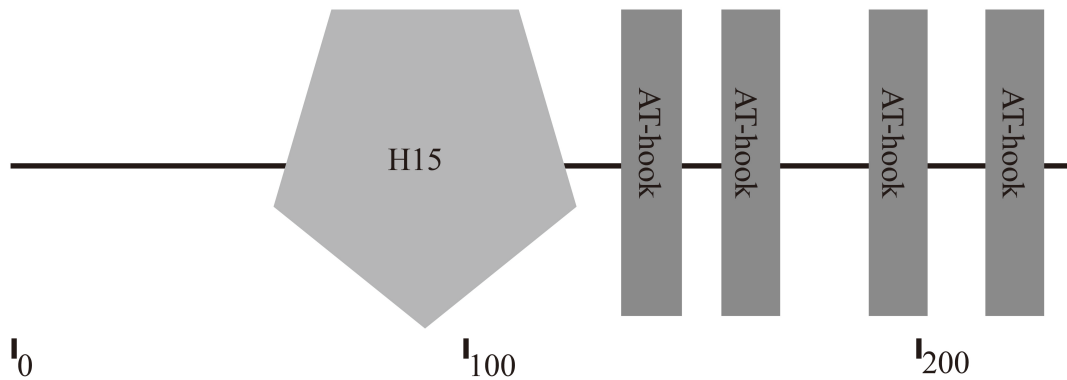
c



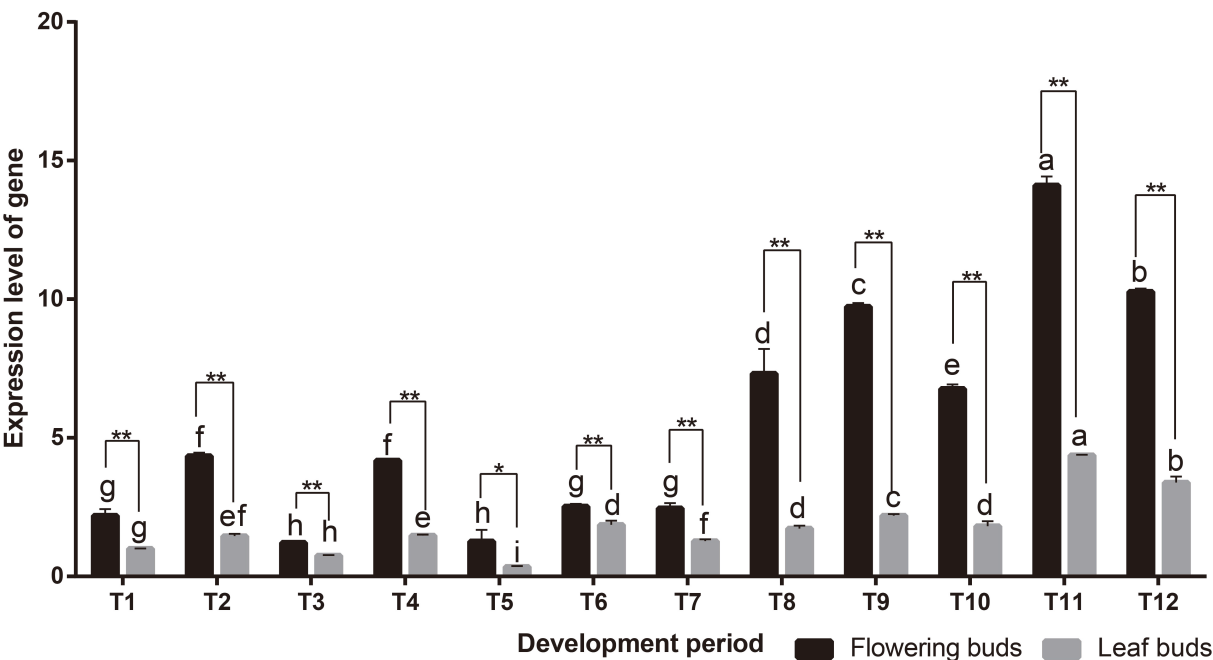
d

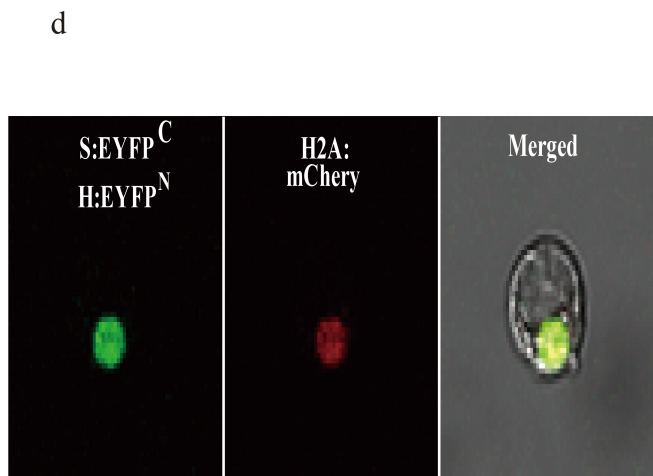
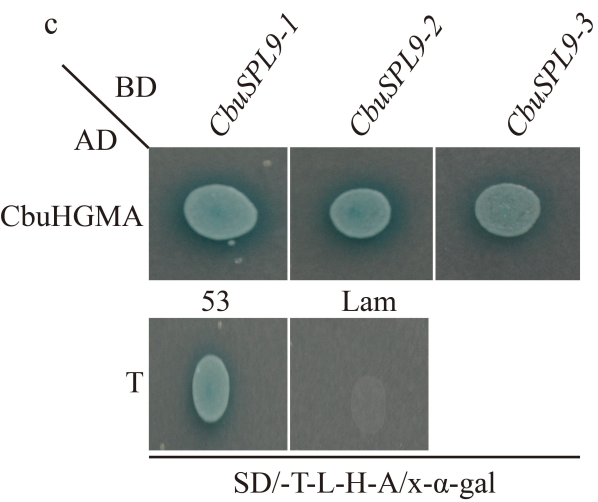
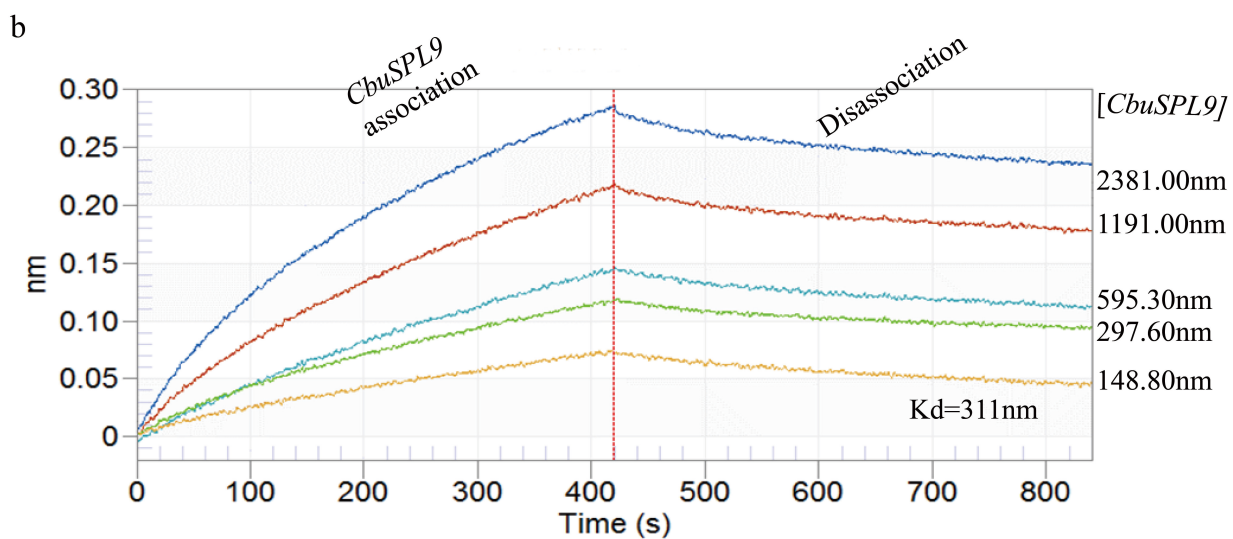
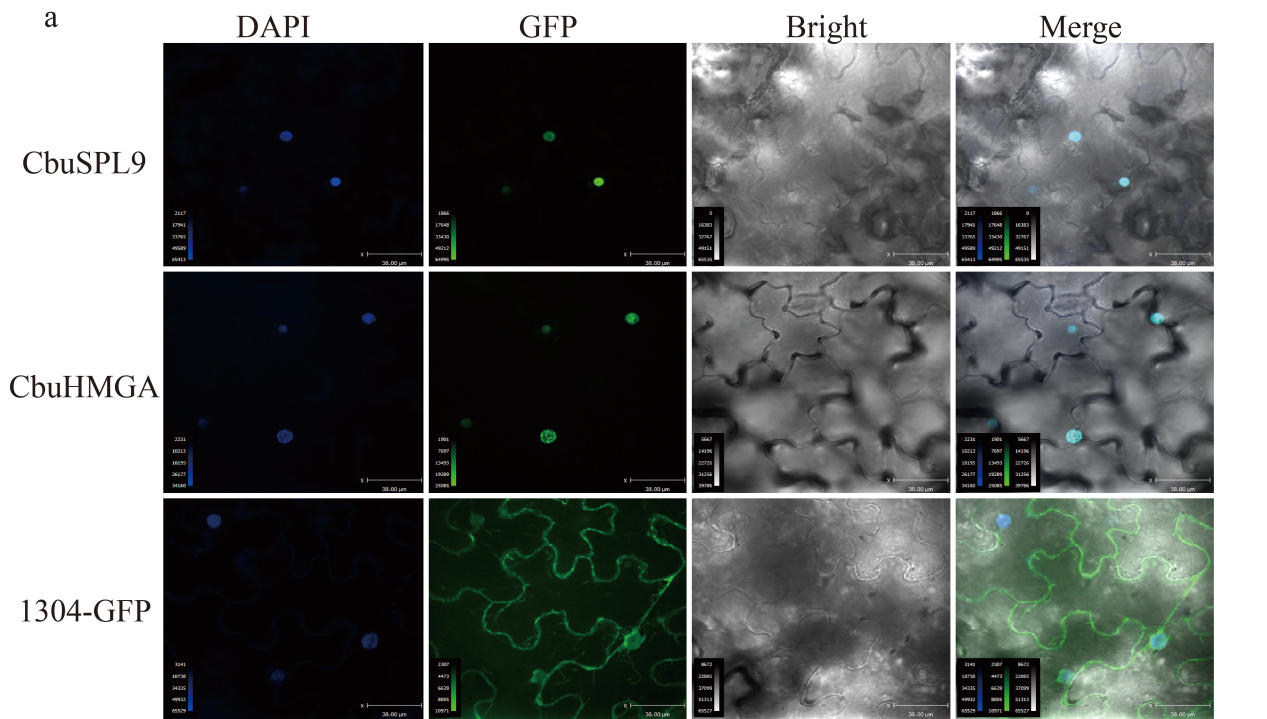


a

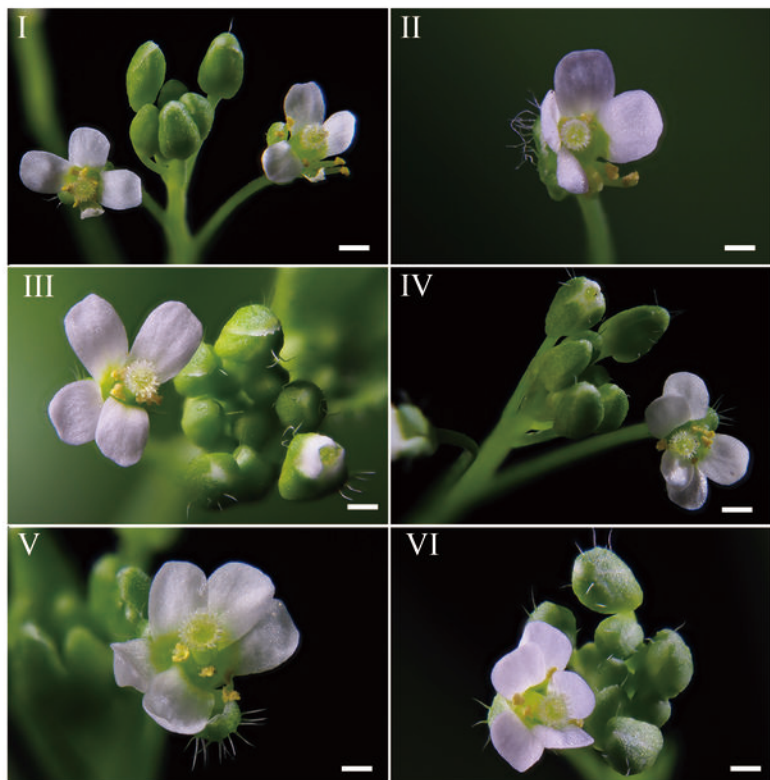


b

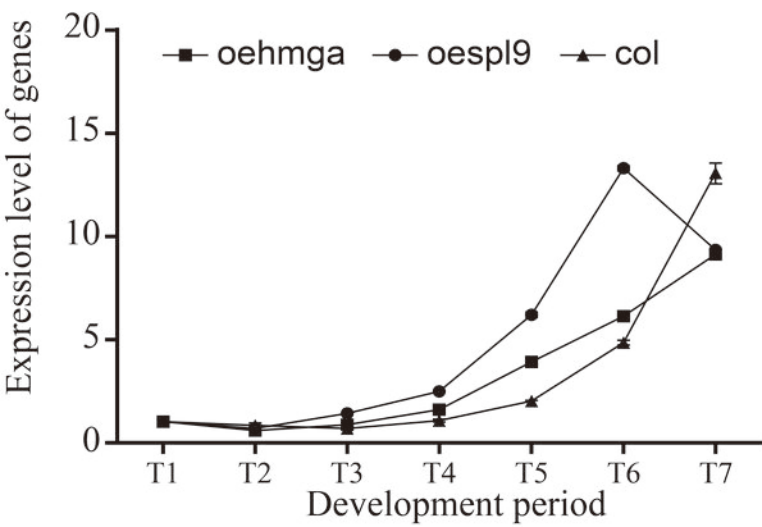




a



b









**Supplementary Table S1 The list of the all Primers used in this paper.**

	Gene name	Primer sequence (5'-3')
Primers used in homology-based cloning of SPL and RACE of homologous gene CbuSPL	SPLF	CAGGTGGAGGGTTGTAAGGT
	SPLR	CCAAGACTCAAGGATCGGGT
	3'RSPLF1	GCAAAGGTTTTGCCAGCAGTG
	3'RACE Out	TACCGTCGTTCCACTAGTGATTT
	3'RSPLF2	CGCCTTGCTGGCCATAACGAGCGTA
	3'RACE Inner	CGCGGATCCTCCACTAGTGATTTCACTATAGG
	5'RSPLR1	AGAAGAGAGAGAGCACCGGTG
	5'RACE Out	CATGGCTACATGCTGACAGCCTA
	5'RSPLR2	CCTGATATGGAAGTTGATACTTT
	5'RACE Inner	CGCGGATCCACAGCCTACTGATGATCAGTCGATG
Primers used in PCR of cDNA from homologous gene CbuSPL9 and CbuHMGA	QCCbuSPLF	ATGCACTGATTGTATGAGGGAG
	QCCbuSPLR	GACACACAGAAAGCAACAACAT
	CbuSPL9F	ATGGAAAAGGGTTCTTCCTC
	CbuSPL9R	TCAGATAGAGGATTTTGTGAGTTT
Primers used in overexpression analysis	CbuHMGA F	ATGGCGAGCGAAGAAGTACA
	CbuHMGA R	CTACAATGATCCATAAATTAATAAAAC
	121CbuSPL9F	TCTAGAATGGAAAAGGGTTCTTCCTC
	121CbuSPL9R	CCTAGGTCAGATAGAGGATTTTGTGAGTTT
Primers used in analysis for the presence of the transgene	121CbuHMGA F	TCTAGAATGGCGAGCGAAGAAGTACA
	121CbuHMGA R	CCTAGGCTACAATGATCCATAAATTAATAAAAC
	CbuSPL9F	GCCATCATTGCGATAAAGGAAA
	CbuSPL9R	ATCCAGACTGAATGCCACAGG
Primers used in subcellular localization analysis	CbuHMGA F	GCCATCATTGCGATAAAGGAAA
	CbuHMGA R	ATCCAGACTGAATGCCACAGG
	CbuSPL9-GFPF	CCATGGATGGAAAAGGGTTCTTCCTC
	CbuSPL9-GFPR	TCTAGATCAGATAGAGGATTTTGTGAGTTT
	CbuHMGA-GFPF	CCATGGATGGCGAGCGAAGAAGTACA
Primers used in yeast two-hybrid	CbuHMGA-GFPR	TCTAGACTACAATGATCCATAAATTAATAAAAC
	BD-CbuSPL9F	CATATGATGGAAAAGGGTTCTTCCTCCT
	BD-CbuSPL9R	GTCGACGTCAGATAGAGGATTTTGTGAGTTTCC
	AD-CbuHMGA F	CATATGATGGCGAGCGAAGAAGTACA
	AD-CbuHMGA R	GTCGACGCTACAATGATCCATAAATTAATAAAAC
Primers used in prokaryotic expression	CbuSPL9-6P-F	GGATCCATGGAAAAGGGTTCTTCCTC
	CbuSPL9-6P-R	CTCGAGTCAGATAGAGGATTTTGTGAGTTT

	Gene name	Primer sequence (5'-3')
ssion	CbuHMGA-HIS-F	CGCGGATCCATGGCGAGCGAAGAAGTACAG
	CbuHMGA-HIS-R	CGCAAGCTTCTAAGCCCCTACGGGTGCGGC
	CbuSPL9F	CACCATGGAAAAGGGTTCTTCCTCCTC
	CbuSPL9R	AAGTGACCAGTGCACAGAAGAATC
Primers used in BIFC	CbuHMGAF	CACCATGGCGAGCGAAGAAGTACAGG
	CbuHMGAR	AGCCCCTACGGGTGCGG
	M13F	GTTGTAAAACGACGGCCAG
	M13R	CAGGAAACAGCTATGAC
	CaMV35S-F	GACGCACAATCCCACTATCC

**Supplementary Table S2 Details of motif-sequences of CbuSPL9 were identified by MEME**

No.	Sequence (5'-3')	Quantity of motif site
1	YYCRHKVCGMHSKSPKVIVAGLEQRFCQQCSRFBHQLPEFD QGKRSCRRRL	16
2	RCQVEGCKVDLSDAK	16
3	AGHNERRRKP	16
4	RTGRIVFKLFGKEPNEFPVLRGQILDWLSHSPTDMESYIRP GCIVLTIY	4
5	PAGLTPLHIAAGKDGSEDVLDALTEDPAMVGIEAWKTCRD STGFTPEDIA	3
6	LGLKLGKRTYFEDFW	7
7	AYRPAMLSMVAIAAVCVCVALLFKSCPEVLYVFQ	3
8	FFPFLVVEDDDVCSEIRILETTLEFTGTDSAKQAMDFIHEIG WLLHR	2
9	FPLIRFQWLIEFSMDREWCAVIRKLLNMFFD	3
10	QAETAWEELSDDLGFSLGKLLDLSDDPLWTTGWYVVRVQN QLAFVYNGQV	3
11	GKRSVEWDLNDWKWD	5
12	ATLSELCLLHRAVRKNSKPMVEMLLRY	5
13	EKAQFTVKGMNLRQRGTRLLCSVEGKYLIQETT	4
14	GRDSWPNTTSEGLGNQSATTGKYQLPYQGNSQNP	2
15	DHHHQRRQYMEDENTRAYDSSSHHTNW	2
16	VNFSCDMPILSGRGFMEIEDQ	2
17	FDNHSRSGGFMMDFSAY	2
18	MECNAKPPFQWELENLISFGTSTAEPVPRKPKMEWEI	2
19	DSNCALSLLSN	7
20	DDQTSNYMLITLLKILSNHSNQSDQ	2

**Supplementary Table S3 Statistics of mutant of floral organs in *oe-SPL9* Arabidopsis**

Type	overlapping petals	Change in petals number	shrunken petals
CbuSPL9-1	-	*	*
CbuSPL9-2	-	*	-
CbuSPL9-3	-	-	-
CbuSPL9-4	*	-	-
CbuSPL9-5	-	*	-
CbuSPL9-6	*	-	-
CbuSPL9-7	*	*	-
CbuSPL9-8	-	*	-
CbuSPL9-9	-	-	-
CbuSPL9-10	-	-	*
CbuSPL9-11	*	*	-
CbuSPL9-12	-	*	*
CbuSPL9-13	*	*	-
CbuSPL9-14	*	*	-
CbuSPL9-15	-	-	*
CbuSPL9-16	-	-	*
CbuSPL9-17	*	*	-
CbuSPL9-18	*	-	-
CbuSPL9-19	-	*	-
CbuSPL9-20	-	*	-
CbuSPL9-21	-	-	*
CbuSPL9-22	-	-	-
CbuSPL9-23	-	*	-
CbuSPL9-24	-	-	*
CbuSPL9-25	-	*	-
CbuSPL9-26	-	*	*
CbuSPL9-27	*	-	-
CbuSPL9-28	-	*	-
CbuSPL9-29	*	*	-
CbuSPL9-30	-	*	-
CbuSPL9-31	-	-	*
CbuSPL9-32	*	-	-
CbuSPL9-33	-	*	-
CbuSPL9-34	-	-	*
CbuSPL9-35	*	*	-
CbuSPL9-36	-	*	-

**Supplementary Table S4 Statistics of mutant of flowering time in *oe-SPL9* Arabidopsis**

Type	DAY	Type	DAY
CbuSPL9-01	22	WT-01	27
CbuSPL9-02	17	WT-02	27
CbuSPL9-03	23	WT-03	26
CbuSPL9-04	21	WT-04	27
CbuSPL9-05	22	WT-05	25
CbuSPL9-06	16	WT-06	28
CbuSPL9-07	22	WT-07	28
CbuSPL9-08	23	WT-08	26
CbuSPL9-09	23	WT-09	25
CbuSPL9-10	22	WT-10	27
CbuSPL9-11	21	WT-11	25
CbuSPL9-12	22	WT-12	27
CbuSPL9-13	23	WT-13	27
CbuSPL9-14	22	WT-14	26
CbuSPL9-15	22	WT-15	27
CbuSPL9-16	24	WT-16	27
CbuSPL9-17	22	WT-17	25
CbuSPL9-18	18	WT-18	29
CbuSPL9-19	23	WT-19	27
CbuSPL9-20	21	WT-20	28
CbuSPL9-21	24	WT-21	27
CbuSPL9-22	23	WT-22	26
CbuSPL9-23	21	WT-23	26
CbuSPL9-24	24	WT-24	27
CbuSPL9-25	21	WT-25	27
CbuSPL9-26	23	WT-26	25
CbuSPL9-27	21	WT-27	26
CbuSPL9-28	18	WT-28	26
CbuSPL9-29	21	WT-29	27
CbuSPL9-30	20	WT-30	26

**Supplementary Table S5 Statistics of mutant of floral organs in *oe-HMGA* Arabidopsis.**

Type	Overlapping petals	Change in petals number	shrunken petals
CbuHMGA-1	*	*	
CbuHMGA-2			*
CbuHMGA-3		*	
CbuHMGA-4	-	-	-
CbuHMGA-5		*	*
CbuHMGA-6		*	
CbuHMGA-7	*	*	
CbuHMGA-8		*	
CbuHMGA-9			*
CbuHMGA-10	*	*	
CbuHMGA-11	-	-	-
CbuHMGA-12	*	*	
CbuHMGA-13		*	
CbuHMGA-14		*	
CbuHMGA-15			*
CbuHMGA-16		*	
CbuHMGA-17		*	*
CbuHMGA-18		*	
CbuHMGA-19	-	-	-
CbuHMGA-20	-	-	-
CbuHMGA-21		*	
CbuHMGA-22	*		
CbuHMGA-23			*
CbuHMGA-24		*	
CbuHMGA-25			*
CbuHMGA-26	*	*	
CbuHMGA-27			*
CbuHMGA-28	-	-	-
CbuHMGA-29			*
CbuHMGA-30	*	*	
CbuHMGA-31			*
CbuHMGA-32		*	
CbuHMGA-33			*
CbuHMGA-34		*	
CbuHMGA-35	-	-	-
CbuHMGA-36	*	*	



**Supplementary Table S6 Statistics of mutant of flowering time in *oe-HMGA* Arabidopsis.**

Type	Time	Type	Time
CbuHMGA-01	25	WT-01	27
CbuHMGA-02	25	WT-02	27
CbuHMGA-03	26	WT-03	26
CbuHMGA-04	24	WT-04	27
CbuHMGA-05	27	WT-05	25
CbuHMGA-06	28	WT-06	28
CbuHMGA-07	26	WT-07	28
CbuHMGA-08	24	WT-08	26
CbuHMGA-09	28	WT-09	25
CbuHMGA-10	27	WT-10	27
CbuHMGA-11	24	WT-11	25
CbuHMGA-12	28	WT-12	27
CbuHMGA-13	27	WT-13	27
CbuHMGA-14	26	WT-14	26
CbuHMGA-15	25	WT-15	27
CbuHMGA-16	28	WT-16	27
CbuHMGA-17	25	WT-17	25
CbuHMGA-18	24	WT-18	29
CbuHMGA-19	28	WT-19	27
CbuHMGA-20	27	WT-20	28
CbuHMGA-21	26	WT-21	27
CbuHMGA-22	26	WT-22	26
CbuHMGA-23	26	WT-23	26
CbuHMGA-24	25	WT-24	27
CbuHMGA-25	27	WT-25	27
CbuHMGA-26	25	WT-26	25
CbuHMGA-27	27	WT-27	26
CbuHMGA-28	26	WT-28	26
CbuHMGA-29	26	WT-29	27
CbuHMGA-30	28	WT-30	26